G Model
FUSION-9622; No. of Pages 6

ARTICLE IN PRESS

Fusion Engineering and Design xxx (2017) xxx–xxx

Contents lists available at ScienceDirect

Fusion Engineering and Design

journal homepage: www.elsevier.com/locate/fusengdes

Numerical simulation of detached plasma in the end-cell of GAMMA 10/PDX for divertor simulation study

M.S. Islam [a,*], Y. Nakashima [a], A. Hatayama [b], K. Ichimura [c], M.M. Islam [a], K. Fukui [a], M. Ohuchi [a], T. Yokodo [a], G. Lee [a], S. Togo [a], N. Ezumi [a], M. Sakamoto [a], T. Imai [a]

[a] *Plasma Research Center, University of Tsukuba, Tsukuba, Ibaraki 305-8577, Japan*
[b] *Graduate School of Science and Technology, Keio University, Yokohama, Kanagawa 223-8522, Japan*
[c] *Department of Electrical and Electronic Engineering, Kobe University, Kobe, Hyogo 657-8501, Japan*

HIGHLIGHTS

- This research investigates the effect of Argon (Ar) and Neon (Ne) injection on the plasma parameters in the end-cell of GAMMA 10/PDX numerically by using a multi-fluid code.
- Temperature reduction in the electrons and ions during Ar injection is higher than those of the Ne injection.
- Particularly in the electron temperature a remarkable reduction is observed during Ar injection.
- The electron density shows a tendency of roll-over phenomenon for Ar injection.
- It is also observed that the radiative power loss due to the Ar injection is much higher than that of the Ne injection.

ARTICLE INFO

Article history:
Received 23 November 2016
Received in revised form 22 May 2017
Accepted 29 May 2017
Available online xxx

Keywords:
GAMMA 10/PDX
D-module
Plasma detachment
Multi-fluid code

ABSTRACT

This research investigates the effect of Argon (Ar) and Neon (Ne) injection on the plasma parameters in the end-cell of GAMMA 10/PDX numerically by using a multi-fluid code. Reduction in the temperature of the electrons and ions is observed according to the increment of impurity injection. The electron density and the particle flux show tendency of roll-over phenomena for Ar injection. Temperature reduction in the electrons and ions during Ar injection is higher than those of the Ne injection. It is also observed that the charge-exchange (CX) loss and radiative power loss for Ar injection is higher than that of the Ne injection. These outcomes indicate that Ar is more effective radiative gas for generating detached plasma.

1. Introduction

In plasma-fusion devices, high heat-load onto the target plates of the divertor is one of the most important issues. Erosion and sputtering are produced on the target plate due to the high heat-load. Therefore, evaluation of plasma cooling mechanism and formation of detached plasma is necessary. It is very important to understand the physical mechanism of plasma detachment. The electron temperature in the divertor region can be reduced if the divertor plasma is seeded with radiative impurities (Such as Ne, Ar, etc.). It is also important to extract the plasma energy from ions by enhanced charge-exchange (CX) collisions. The plasma temperature can further be decreased due to the recycling hydrogen atoms and molecules near the target plate. In addition, Electron-ion recombination (EIR) [1] and molecular activated recombination (MAR) [2] processes in divertor plasmas are also very much important to achieve plasma detachment.

GAMMA 10/PDX is the world's largest linear device which is 27 m in length. GAMA 10/PDX consists of central-cell, anchor-cells, plug/barrier-cells and end-cells [3]. The typical plasma parameters of GAMMA 10/PDX in the central-cell are $T_{i\|} \sim 400$ eV, $T_e \sim 50$ eV, and $n_e \sim 2 \times 10^{18}$ m^{-3} [4]. The end-loss plasmas of GAMMA 10/PDX escape from the central-cell and then transport through the anchor-cell, subsequently to the plug/barrier-cell and finally reach at the end-cell. Study of the end-loss flux of GAMMA 10/PDX is an important research areas for studying plasma-divertor interaction simulation experiments [5,6]. In GAMMA 10/PDX, divertor simula-

* Corresponding author.
E-mail addresses: shahinul@prc.tsukuba.ac.jp, shahinulislamrony@gmail.com (M.S. Islam).

http://dx.doi.org/10.1016/j.fusengdes.2017.05.132
0920-3796/

Please cite this article in press as: M.S. Islam, et al., Numerical simulation of detached plasma in the end-cell of GAMMA 10/PDX for divertor simulation study, Fusion Eng. Des. (2017), http://dx.doi.org/10.1016/j.fusengdes.2017.05.132

tion experiments have been started by using a divertor simulation experimental module (D-module) in which a V-shaped target made of tungsten has been installed [4]. It has been aimed to investigate the physics of plasma detachment and radiation cooling. In order to investigate the physics of plasma detachment and radiation cooling, several radiator gases (Ne, Ar, Xe and N_2) have been injected into the D-module of GAMMA 10/PDX [7–10].

Numerical simulation study is a very useful tools to understand the physical mechanism of plasma detachment, impurity transport, etc. The fluid code which simulates Scrape-off Layer (SOL) plasma is widely used in the world such as B2 [11] and B2.5 [12]. A numerical simulation study by using a multi-fluid code [13,14] has been started in order to understand the physics of plasma detachment and energy loss processes in GAMMA 10/PDX. The present multi-fluid code has been developed based on the B2-code, which has been originally developed by B.J. Braams for the numerical simulation of tokamak SOL and divertor plasmas [11].

In order to investigate the energy loss processes, atomic processes of hydrogen, Ne and Ar [15,16] are included in the present code. In addition, recycling hydrogen atoms near the target plate are also included in the present model. The purpose of this study is to investigate the physics of plasma detachment in the case of radiator gases (Ar and Ne) injection in the end-cell of GAMMA 10/PDX numerically.

Section 2 describes the mesh structure of the simulation area. Physical model of the code is described in section 3. Simulation results and discussions are described in section 4. A brief summary of the principle results and future plans is described in section 5.

2. Mesh structure

At the current numerical model, the numerical meshes are created on the basis of the GAMMA10/PDX magnetic field configuration by approximately the same manner as the B2 code [11]. The current simulation model assumes the axial symmetry and 2D model in the x and y direction, while physical quantities are assumed to be uniform in the theta (θ) direction. The x-direction and y-direction in the local orthogonal coordinate system correspond to the direction of parallel and perpendicular to the magnetic field, respectively. Fig. 1 shows the numerical mesh model. In this model, the mesh structure is constructed in such a way that each cell becomes a rectangle shape with its sides being locally orthogonal to each other.

As shown in Fig. 1, a tungsten (W) target is assumed to be located at the end of the mesh structure. Furthermore, the calculation area in the radial (r axis) direction is 0∼0.15 m (50 cells) from the center axis of GAMMA10/PDX. On the contrary, the calculation area in the axial (z axis) direction is 7.50–10.70 m (321 cells) i.e. from the plug/barrier to the end-cell of GAMMA10/PDX.

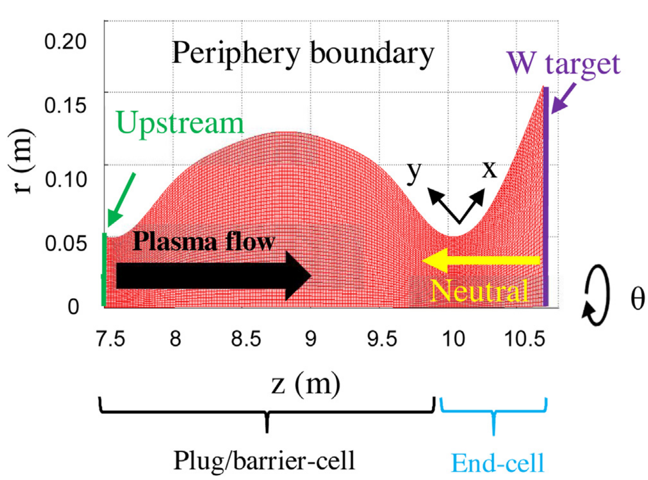

Fig. 1. Mesh structure of the simulation area.

3. Physical model

The multi-fluid code consists of the following five equations: continuity equation, parallel momentum equation, diffusion approximation for the flux across the magnetic field, ion energy-balance equation and electron energy-balance equation. Multi-fluid model including the impurity ions is used in the following analyses.

Continuity equation of ion species α;

$$\frac{\partial n_\alpha}{\partial t} + \frac{\partial}{\partial x}(n_\alpha u_\alpha) + \frac{\partial}{\partial y}(n_\alpha v_\alpha) = S_n^\alpha \tag{1}$$

The symbol S_n^α is associated with ionization and recombination.

Diffusion equation of species α in the radial direction;

$$v_\alpha = -D_n^\alpha \frac{\partial}{\partial y}(\ln n_\alpha). \tag{2}$$

D_n^α is the Bohm diffusion coefficient.

Momentum balance equation of ion species α;

$$\begin{aligned}
&\frac{\partial}{\partial t}(m_\alpha n_\alpha u_{||\alpha}) + \frac{\partial}{\partial x}\left(m_\alpha n_\alpha u_{||\alpha} u_\alpha - \eta_x^\alpha \frac{\partial u_{||\alpha}}{\partial x}\right) + \frac{\partial}{\partial y}\left(m_\alpha n_\alpha u_{||\alpha} v_\alpha - \eta_y^\alpha \frac{\partial u_{||\alpha}}{\partial y}\right) \\
&= \frac{B_\theta}{B}\left[-\frac{\partial p_\alpha}{\partial x} - \frac{Z_\alpha n_\alpha}{n_e}\frac{\partial p_e}{\partial x} + c_e\left(\frac{Z_\alpha}{Z_{eff}} - 1\right) Z_\alpha n_e \frac{\partial T_e}{\partial x} + c_i\left(\frac{Z_\alpha}{Z_{eff}} - 1\right) Z_\alpha n_\alpha \frac{\partial T_i}{\partial x}\right] \\
&+ \sum_{\beta=1}^{N} F_{\alpha\beta} + S^\alpha_{\mathbf{mu}||}.
\end{aligned} \tag{3}$$

The source and sink terms associate with CX loss between H^+ and H^0, and recombination are denoted by $\boldsymbol{S^\alpha_{mu||}}$.

Electron energy balance equation;

$$\begin{aligned}
&\frac{\partial}{\partial t}\left(\frac{3}{2} n_e T_e\right) + \frac{\partial}{\partial x}\left(\frac{5}{2} n_e u_e T_e - \kappa_x^e \frac{\partial T_e}{\partial x}\right) + \frac{\partial}{\partial y}\left(\frac{5}{2} n_e v_e T_e - \kappa_y^e \frac{\partial T_e}{\partial y}\right) \\
&= u_e \frac{\partial p_e}{\partial x} + v_e \frac{\partial p_e}{\partial y} - k(T_e - T_i) - k_z(T_e - T_z) + \boldsymbol{S_E^e}.
\end{aligned} \tag{4}$$

The symbol $\boldsymbol{S_E^e}$ is associated with ionization, recombination and radiative power loss of Ar and Ne.

Ion energy balance equation;

$$\begin{aligned}
&\frac{\partial}{\partial t}\left(\frac{3}{2} n_i T_i + \sum_\alpha \frac{1}{2}\rho_\alpha u_{||\alpha}^2\right) + \frac{\partial}{\partial x}\left[\left(\sum_\alpha \frac{5}{2} n_\alpha u_\alpha T_i + \sum_\alpha \frac{1}{2} m_\alpha n_\alpha u_\alpha u_{||\alpha}^2\right)\right. \\
&\left. - \left(\kappa_x^i \frac{\partial T_i}{\partial x} + \sum_\alpha \frac{1}{2}\eta_x^\alpha \frac{\partial u_{||\alpha}^2}{\partial x}\right)\right] \\
&+ \frac{\partial}{\partial y}\left[\left(\sum_\alpha \frac{5}{2} n_\alpha v_\alpha T_i + \sum_\alpha \frac{1}{2} m_\alpha n_\alpha v_\alpha u_{||\alpha}^2\right) - \left(\kappa_y^i \frac{\partial T_i}{\partial y} + \sum_\alpha \frac{1}{2}\eta_y^\alpha \frac{\partial u_{||\alpha}^2}{\partial y}\right)\right] \\
&= -u_e \frac{\partial p_e}{\partial x} - v_e \frac{\partial p_e}{\partial y} + k(T_e - T_i) + S_E^I + \sum_{\alpha\beta} F_{\alpha\beta}(u_{||b} - u_{||a}).
\end{aligned} \tag{5}$$

The symbol $\boldsymbol{S_E^I}$ is associated with CX loss between H^+ and H^0, and recombination.

Here the following notations are used: n_e and n_i are the density of electrons and ions; m_α and Z_α are the mass and charge number of species α; v_e and v_i are the velocity of electron and ion; T_e and T_i are the electron and ion temperatures; p_e is the pressure of electrons;